Hypersensitive Transitions: A Greener Micellar Study of Tb(III)-Indole Derivative Complexes through Optical Absorption Spectra

Ramswaroop Regar[1]*, Sumit Ghasia[2], Hemendra Singh Bhandari[3]

[1]Assistant Professor, P.G. Department of Chemistry, SK Government Girls College, Sikar (India)
*Corresponding author: ramswaroopregar06[at]gmail.com
[2]Assistant Professor, P.G. Department of Chemistry, SK Government Girls College, Sikar (India)
ghasiasumit[at]gmail.com
[3]Assistant Professor, GCRC, P.G. Department of Chemistry, Govt. Dungar College, Bikaner, (India)
hsbhandari78[at]gmail.com

Abstract: *Optical absorption spectra of Terbium(III)-complexes with Nitrogen and Oxygen containing ligand Indole derivative [viz : 1H-indole-3-carboxylic acid (I3CA), 1-(1H-indole-3-yl)ethanone (3ATI) and 1H-indole-3-carbaldehyde (I3CD)] have been studied and analyzed in non-micellar solvent (Alcohol+water) as well as micellar surfactant medium [Polyethylene glycol monododecyl ether (BRIJ35), Cetyltrimethylammonium bromide (CTAB), Sodium dodecyl sulphate (SDS)] at 298 K temperature. UV-Visible absorption spectra of metal-ligand complexes produce eight multiplet to multiplet transition bands in 250-400 nm range. These transitions are originated from $^7F_6$ ground state and obtained as $^5H_6 \leftarrow {}^7F_6$, $^5H_7 \leftarrow {}^7F_6$, $^5D_1 \leftarrow {}^7F_6$, $^5L_{8,} \leftarrow {}^7F_6$, $^5L_9 \leftarrow {}^7F_6$, $^5G_5 \leftarrow {}^7F_6$, $^5L_{10} \leftarrow {}^7F_6$, $^5G_6 \leftarrow {}^7F_6$ for Terbium(III)- indole derivatives complexes. The transition $^5H_7 \leftarrow {}^7F_6$ is highly sensitive as it has high Oscillator Strength (P) with the non-ionic BRIJ35 micellar medium. The hypersensitivity of transitions and enhancements in spectral peaks is applicable in resolution technique. In this optical absorption study Intensity parameters are studied by applying Judd Ofelt theory. Covalency character are assigned by four covalency parameters β , $b^{1/2}$, δ and η for the studied metal-ligand complexes and found better in green micellar medium. Green micellar solvents are safer for environment.*

Keywords: Oscillator strength, Micellar medium, Hypersensitive transition, Covalency parameters

1. Introduction

The 'Green Chemistry' deals with the utilization of chemical science for better future, safer environment, and maintain the ecological balance. The population of world are increasing exponentially, which creates pressure on the environment in form of adding more harmful and toxic substances to the environment by many physiological, chemical, mechanical, industrial and biological activity [1]-[5]. These adverse effects on environment also increases through the use of solvents in scientific research activity. These adverse effects have to be diminished to a safer level of sustainable environment by the use of green solvents as micellar surfactants in research activity [6]-[9]. The physiochemical properties of metal ion and its organic ligand complexes are affected by various solvent systems, whether these solvents are micellar or non-micellar. This interaction between the metal and ligand also has greater impacts of solvents as changes in physiochemical properties of complexes, in presence of different solvent systems reflects in nature of bonding [10]-[12].

Terbium has applications in fluorescent devices, Vehicle industries, alloys, laser, solid state and electronic devices. For improvement of life span as well as quality of light, many fluorescent devices can be prepared incorporation with terbium like trichromatic lightening, low light bulbs, mercury lamps, color television tubes and color phosphor High-Definition screen [13]-[15]. $TbSO_4$ are used to identify the counterfeiting currency in banks. For this Eu(III), Tb(III) and Tm(III) metal ion produce red, green and blue color on exposure of the UV light [16]-[17]. The presence of microbes is identified by using salt $TbCl_3$. For this, $TbCl_3$ are employed on test area, appearance of green color on applying the UV light assign the presence of microbes or live endospores [18]-[19]. Terbium laser light (solid state devices+ optical fibers) are used in medical surgery, medical equipment's, aerospace and laser printing [20]-[21].

Indole derivatives in various forms have been applied for potential activity against inflammation, Indomethacin for treatment of rheumatoid arthritis, analgesic activity, cluster headache remedies, alcoholism and treatment of pain.[22]-[23]. For targeted cancer therapy, horseradish peroxidase was oxidized with 6-chloro substituted indole-3-acetic acid which was used as prodrugs for enzyme-prodrug. Obtained compound exhibited toxicity against the Chinese hamster V79 lung fibroblast. Halogenated indole-3-acetic acid possesses maximum cytotoxicity against prodrugs and horseradish peroxidase. Toxicity of substituted 3-methylene oxindoles was enhanced in presence of electron withdrawing group [24].

Lanthanide required high energy for excitation in the UV Visible region as the 4f subshell is deeply situated than 5d subshell and surrounded by the 5p and 5s orbitals. Hence, lanthanide shows less metal-ligand interaction with the approaching ligands. The 4f-4f transition of $4f^N$ electrons are Laporte forbidden transitions which occurs due to absorption of radiation in the 200 nm – 800 nm region [25]. Some of 4f-4f transition have high oscillator strength due to different surrounding environment from other transitions are known as hypersensitive transitions. These transitions follow $|\Delta J| \leq 2$, $|\Delta L| \leq 2$, $|\Delta S|=0$ selection rule for 4f-4f transition. Many factors show the variation in hypersensitive transitions like polarization of ligand, mixing of f-d orbitals, charge transfer

ligand to metal, molecular vibration and spin-orbital configuration interaction. [26]

2. Review of Literature

Ahmed Zuber *et al.* synthesized octacoordinated [Tb(hfaa)$_3$(indazole)$_2$], [Lu(hfaa)$_3$(indazole)$_2$], [Dy(hfaa)$_3$(indazole)$_2$] and nine coordinated [Eu(hfaa)$_3$(indazole)$_3$] complexes using a monoanionic bidentate hexafluoroacetylacetone (hffa$^-$) and a neutral monodentate indazole ligand. For synthesis of these complexes, metal: hfaa : indazole ratio were kept 1:3:2 in AR or spectroscopic grade solvent. Efficient energy transfer from ligand→ metal have been determined by photophysical studies in complexes of metal and ligand indazole. Absorption spectroscopy study achieved a strong band at 375 nm due to strong overlapping among metal, ligand hfaa and indazole. [27]. Debnath H G et al. have been synthesized the Zn(Tb)S nanoparticle as function of reaction temperature by incorporation of Tb(III) metal with zinc sulfide. Intra configurational *4f-4f* sharp emission bands were revealed in all studied nanoparticles Zn(Tb)S which was characteristics of Tb(III) metal ion. Absorption spectra of Zn(Tb)S nanoparticles were recorded in ultraviolet and visible light range. New devices of optical material can be developed with help of semiconductor and Ln(III) metals on rationalized and optimized of these studied photophysical properties of Zn(Tb)S nanoparticles [28]. Zhao Yan-Wu et al. have been synthesized [Ln(CPOMBA)(H$_2$O)$_2$]. nH$_2$O complexes by reaction of Ln(NO$_3$)$_3$ and H$_3$CPOMBA. Here, Ln = Gd^{3+}, Tb^{3+}, Ho^{3+}, Tm^{3+}. Furthermore, synthesis of complexes Eu$_{0.045}$Tb$_{0.955}$CPOMBA and La$_{0.6}$Eu$_{0.1}$Tb$_{0.3}$CPOMBA were prepared, based on metal-organic framework which were the single-phase, white-light phosphor near Ultraviolet region. Variation in temperature, solvent and reaction conditions crystals of single phase have been obtained which were stable in air, insoluble in organic solvent and H$_2$O. In these mix complexes of Tb(III) and Eu(III), transfer of energy from organic ligand to rare earth metals takes place. Single-phase ultraviolet phosphor can be developed by utilizing this new approach [29]. Pan Gencai *et al.* have been obtained visible to NIR region tunable multicolor emission, stable and photoluminescence high quantum yield nanocrystals by modified hot-injection method. Absorption spectra revealed the dependance of photoluminescence on concentration of dopant lanthanide. In absorption spectra, the doping ions which possesses higher atomic number, shift the host's first excitation peak towards lower wave length or higher energy. The doping of lanthanide also enhanced the colloidal stability of CsPbX$_3$ perovskite nanocrystals. These dopped nano crystals also exhibition blue shift of energy band gap [30]. Loiko Pavel *et al.* have been evaluated the spectroscopic properties of Tb(III) with polarized light in double tungstate KLu(WO$_4$)$_2$ crystal. For transition of lower state to higher state measurement was done in visible, near and mid-IR region. For polarization of light maximum cross section of absorption was obtained for $^7F_6 \rightarrow {}^5D_4$ transition at wavelength 486.7 nm. Applying the modified Judd Ofelt theory, transition probabilities of Tb(III) have been computed. With the help of absorption spectra, oscillator strength and four modified Judd Ofelt parameters Ω_2, Ω_4, Ω_6 and α for Tb(III) ion with KLu(WO$_4$)$_2$ have been calculated. Smallest root mean square deviation was obtained for

intermediate configuration interaction model over to modified Judd Ofelt theory [31]. Liu Bin et al. have been studied spectroscopic parameters of single crystal of Tb(III) doped YAlO$_3$ by Czochralski method. Spin forbidden as on *4f-4f* transitions attained in lower wave length region while spin allowed transitions in near IR region. $^5D_4 \rightarrow {}^7F_4$ transition was responsible for yellow intense light emission. For yellow laser operation Tb:YAP crystal can be better source for emission [32]. Subrahmanyam T *et al.* have been studied the dopped Tb(III)-oxyfluoro tellurite (TWGTb) glasses to achieved various spectroscopic and radiative parameters applying Judd Ofelt theory. On excitation of 316 nm wavelength, $^5D_3 \rightarrow {}^7F_{5.3}$ and $^5D_4 \rightarrow {}^7F_6$ transition were achieved. It was depicted that emission of highly intense green luminescence light can be gained from host material by adding 1.0 mol % of dopped Tb(III) in oxyfluoro tellurite glasses at 545 nm wavelength. [33].

3. Aspects of Present Research Work

In the present optical absorption study different parameters; oscillator strength, hypersensitive transitions, Judd Ofelt parameters (T$_2$,T$_4$,T$_6$), and covalency bonding parameter of Terbium(III) with few Indole derivatives I3CA, 3ATI and I3CD in non-micellar solvent (Alcohol+Water) and micellar medium BRIJ35, CTAB, SDS have been investigated using Judd Ofelt method. Effect of micellar or non-micellar solvents also studied on hypersensitive transitions. No any earlier evidences were reported in literature about spectral studies and different parameters of Tb(III) cation with I3CA, 3ATI and I3CD Indole derivatives in both non-micellar and micellar surfactant BRIJ35, CTAB and SDS system. The present work has great attention to know the metal-ligand interaction, nature of the metal-ligand bond and effect of solvent on the hypersensitive transitions and various spectral intensity in term of oscillator strength(P) of Tb(III) complexes with Indole derivatives in different environment of micellar and non-micellar system.

4. Experimental

This part includes preparation of different solution of lanthanide metal Terbium, Indole derivative and non-micellar [Alcohol+Water] and micellar BRIJ35, SDS, CTAB surfactant medium for Optical absorption study in spectral range 250 nm–400 nm. For spectral investigation of different metal-ligand solution in different medium, 12 sample sets of each doped metal systems are prepared in 1:3 metal ligand ratio to record the spectra on UV-Visible Double beam Spectrophotometer in the UV-Visible range 250 nm–400 nm. Raw data are used to prepare the electronic spectra graph with the help of Origin Lab software application.

5. Calculations

5.1 Oscillator Strength:-Oscillator strength 'P' is a measure of the intensity of an absorption band. The area under the peak of an absorption spectrum represents oscillator strength 'P' can also expressed in term of ε_{max} and half bandwidth $\Delta V^{1/2}$ [34]-[35]

$$P_{obs} = 4.6 \times 10^{-9} \times \varepsilon_{max} \times \Delta V^{1/2} \qquad (1)$$

$\Delta V^{\frac{1}{2}}$ =half bandwidth of an absorption band

5.2 Judd Ofelt Parameters:-Energy of a transition ῡ in cm^{-1} and square of matrix element $U^{(\lambda)}$ are related with the oscillator strength which is due to an induced electric dipole transition. [34]-[38]

$$P = T_2 \bar{\upsilon} [U^{(2)}]^2 + T_4 \bar{\upsilon} [U^{(4)}]^2 + T_6 \bar{\upsilon} [U^{(6)}]^2 \quad (2)$$

$U^{(2)}, U^{(4)} U^{(6)}$ = Matrix elements

T_2, T_4, T_6 are Judd Ofelt parameters represented in ratio T_4 / T_2 as coordination parameter and ratio T_4 / T_6 as symmetry parameters.

5.3 Covalency Parameters

(i) β: -Nephelauxetic effect β which is used to estimate the "degree of covalency" $\beta = \frac{\bar{\upsilon}_{avarage(complex)}}{\bar{\upsilon}_{avarage(freeion)}}$ (3)
$\bar{\upsilon}_{avarage(complex)}$ = average bond position of complex in absorption spectra inwavenumber cm^{-1}, $\bar{\upsilon}_{avarage(freeion)}$ = average bond position of free ion in absorption spectra in wave number cm^{-1}

(ii) $b^{\frac{1}{2}}$: $-$Expression of metal wave function when covalent bond formation takes place by f- orbitals
$$< \phi_{4f}| = (1-b)^{\frac{1}{2}} < 4f| - b^{\frac{1}{2}} < \phi_{ligands}| \quad (4)$$
$b^{\frac{1}{2}}$ = amount of 4f orbital mixing
Nephelauxetic ratio β and covalency factor correlated as. [39]
$$b^{\frac{1}{2}} = [\frac{1}{2}(1-\beta)]^{\frac{1}{2}} \quad (5)$$

(iii) δ : $-$Sinha expresses the parameter of covalency. [25]-[26], [40]
$$\delta = \frac{(1-\beta)}{\beta} \times 100 \quad (6)$$

The value of β is found positive then it represents covalent bonding in the metal-ligand Complexes while negative value of β represents the ionic bonding in the metal-ligand complexes.

(iv) η : $-$Covalency angular overlap parameter represented as. [41]
$$\eta = \frac{(1-\beta)^{1/2}}{\beta^{1/2}} \quad (7)$$

6. Result and Discussion

Spectroscopic investigation for the solution behavior of lanthanide Tb(III) ion with three Indole derivative ligands I3CA, 3ATI and I3CD doped systems was done in the UV Visible spectral range of 250 nm to 400 nm at room temperature 298 K. Various parameters were exploited on the analysis of electronic spectrum which was obtained by the plotting the absorbance of solution and wavelength in nm. Eight absorption multiplet-to-multiplet transitions bands as $^5H_6 \leftarrow {}^7F_6$, $^5H_7 \leftarrow {}^7F_6$, $^5D_1 \leftarrow {}^7F_6$, $^5L_8 \leftarrow {}^7F_6$, $^5L_9 \leftarrow {}^7F_6$, $^5G_5 \leftarrow {}^7F_6$, $^5L_{10} \leftarrow {}^7F_6$, $^5G_6 \leftarrow {}^7F_6$ for Tb(III) ion with three indole derivatives in all doped systems have been obtained with enhanced intensities and significant shapes [34], [42]. These plots were presented in Figure 1 to 12 after resolving into a Gaussian shaped curve. Absorption spectra of doped systems in all four medium Alcohol+Water, BRIJ35, SDS, CTAB

were represented for Tb(III)-I3CA complexes in Figure 1 to 4, for Tb(III)-3ATI complexes in Figure 5 to 8, for Tb(III)-I3CD complexes in Figure 9 to 12 respectively.

On the analysis of all 12 doped electronic spectra, it was revealed that interaction between metal Tb(III) ion and ligand I3CA, 3ATI, I3CD indole derivative have been obtained in non-micellar and micellar solvents.

Magnitude of experimental P_{exp} and computed P_{cal} oscillator strength was also obtained for Tb(III) metal with I3CA, 3ATI and I3CD doped systems for comparative analysis of intensity parameter of various electronic transitions. Oscillator strength experimental as well as theoretically have been tabulated in Table-1 and -2.

Previous literature witnesses regarding to experimental oscillator strength P_{exp} and measurement of intensity of various transitions it was observed that few transitions among all transitions, supposed to be very much sensitive to the surrounding environment of metal ion was named as "hypersensitive transitions". Analysis of spectra and computed data, a correlation was well established in between intensity enhancement of hypersensitive transitions and increase of coordination number [36], [43]-[45]. Present study revealed that the hypersensitive and other transitions dramatically found to be greater magnitude of oscillator strength in micellar medium over to non-micellar.

The transitions of greater oscillator strength were observed in all 12 doped systems as $^5H_7 \leftarrow {}^7F_6$ for complex Tb(III)-I3CA, $^5L_9 \leftarrow {}^7F_6$ for complex Tb(III)-I3CA and $^5H_6 \leftarrow {}^7F_6$ transition for complex Tb(III)-I3CA all in BRIJ35 medium. Order of these intensified transitions were obtained as $^5H_7 \leftarrow {}^7F_6 > {}^5L_9 \leftarrow {}^7F_6 > {}^5H_6 \leftarrow {}^7F_6$ for all complexes of Terbium with indole derivative. Here, $^5H_7 \leftarrow {}^7F_6$ transition (Oscillator strength=17.25817939) have been found to be most intensified and hypersensitive transition represented in Figure 2.

The magnitude of oscillator strength was product of ε_{max} and half band width. Enhanced oscillator strength of hypersensitive transitions can also be corelated with the matrix element of that particular transition. The *f-f* transition $^5H_7 \leftarrow {}^7F_6$, as higher magnitude of oscillator strength as it has high value of matrix element ($U^{(2)} = 0.0060$, $U^{(4)} = 0.0019$, $U^{(6)} = 0.0131$), whereas f-f transition $^5L_8 \leftarrow {}^7F_6$, has the lowest magnitude of oscillator strength since its matrix element has lowest value ($U^{(2)} = 0.0$, $U^{(4)} = 0.0001$, $U^{(6)} = 0.0235$). [46]-[49] It was observed that magnitude of oscillator strength depends upon the wavelength of particular *f-f* transition. Irradiation of higher wavelength result out the lower magnitude of oscillator strength.

The augmentation of ε_{max} and oscillator strength was demonstrated via metal-ligand interaction. In BRIJ35 cationic micellar medium, the highest oscillator strength (17.25817939) was found in Tb(III)-I3CA complex.

An increase in ε_{max} and oscillator strength was produced better outcomes in micellar medium over to non-micellar medium. Root mean square deviation σ (r.m.s) have been computed for the experimental P_{exp} and calculated P_{cal}

oscillator strength. Maximum value (8.342630027) of σ (r.m.s) was assigned for Tb(III)-I3CA in BRIJ35 medium while least (2.7849744) for Tb(III)-3ATI in Alcohol+Water medium. The low value of σ (r.m.s) was significant which shown the proximity and validation of obtained data for Terbium(III) with indole derivative systems doped study.

By the incorporation of value of matrix element and experimental value of oscillator strength in equation (2), the T_λ Judd Ofelt parameter was obtained as three sets of T_2, T_4, T_6 parameters [47], [50]-[51]. Computed value of parameter T_2, T_4, T_6 was represented in Table-3. High value of the T_2 parameter was obtained in complex Tb(III)-I3CA in SDS (T_2=549.2388943), Tb(III)-I3CA in BRIJ35 micellar and Tb(III)-I3CA in Alcohol+Water. On this basis it was concluded that Judd Ofelt parameter T_2 exhibited micellar sensitivity. T_2 value for all complexes have a positive value which established the existence of covalency between the metal Tb and Indole derivatives. Highest value (165.1101143) of T_4 parameter was obtained for the complex Tb(III)-I3CD in BRIJ35 micellar medium while the least magnitude (2.020558293) was obtained for Tb(III)-I3CA in CTAB micellar medium. Complex Tb(III)-I3CA in Alcohol+Water exhibited highest value (19.94447329) of T_6 parameter while Tb(III)-I3CA in SDS exhibited lowest value (0.10161281). The T_4/T_2 ratio of Judd Ofelt parameters known as coordination parameters, was obtained essentially constant, resulting that the Tb(III) ion was surrounded by the same coordination environment. Magnitude of T_4/T_2 ratio was obtained highest for the Tb(III)-I3CD in BRIJ35 micellar medium while least for Tb(III)-I3CA in BRIJ35 medium. As a result, the Indole derivatives I3CA, 3ATI and I3CD was generated the same coordination environment around the Tb(III) ion. The values of symmetry parameter T_4/T_6 ratio exhibited great variability which indicated that the symmetry of central metal Tb(III) ions have been changed. Magnitude of T_4/T_6 ratio was obtained highest for the Tb(III)-I3CA in SDS micellar medium while least for Tb(III)-I3CA in Alcohol+Water medium. Covalency parameters have been computed, analyzed and presented in the Table-4 viz: Nephelauxetic ratio (β), Bonding Parameter ($b^{1/2}$), Sinha's covalency parameter δ and Covalency angular overlap parameter (η) for all Tb(III)-indole derivative doped systems. In the solution phase, interaction of Tb metal and N, O donor coordinating ligand was observed as the result of decrease in interelectronic repulsion parameter. In absorption spectra, maximum red shift (β= 0.987408443) as nephelauxetic ratio was observed in SDS anionic micellar medium for Tb(III)-I3CA. Nephelauxetic ratio β is less than one, revealing a red shift in electronic transition spectra. More deviation from unity (< 1) exerted greater nephelauxetic effect β. Minimum red shift ((β= 0.99527125) was obtained for Tb(III)-I3CA in CTAB micellar medium. Higher extent of mixing of 4f orbital represented by $b^{1/2}$ and have been delineated as greater magnitude of red shift. Maximum $b^{1/2}$ was computed 0.079345941 while minimum 0.04862485. Sinha's covalency factor δ maximum was computed 1.275212577 while 0.47512203 as lowest. Covalency angular overlap parameter η obtained maximum 0.006355864 while lowest 0.0023728 which assigned the covalent bonding in interacting species Tb(III) ion and indole derivatives I3CA, 3ATI and I3CD.

On above discussion and computed value, it was assigned that all the four covalency parameters β, $b^{1/2}$, δ and η were obtained maximum in significant magnitude for Tb(III)-I3CA in SDS micellar medium while minimum for Tb(III)-I3CA in CTAB medium. Interaction among the complexes of Tb(III) ion and indole derivatives, surrounding coordination environment, symmetry of Tb(III) ion and covalency character in complexes have been interpreted through analysis of electronic spectra, computed Judd Ofelt parameters and covalency parameters as compare to free Tb(III) ion in both non-micellar and micellar medium. The covalent character among the studied lanthanide Tb metal-ligand complexes was assigned as the shifting of absorption bands towards higher wavelengths or lower wave number.
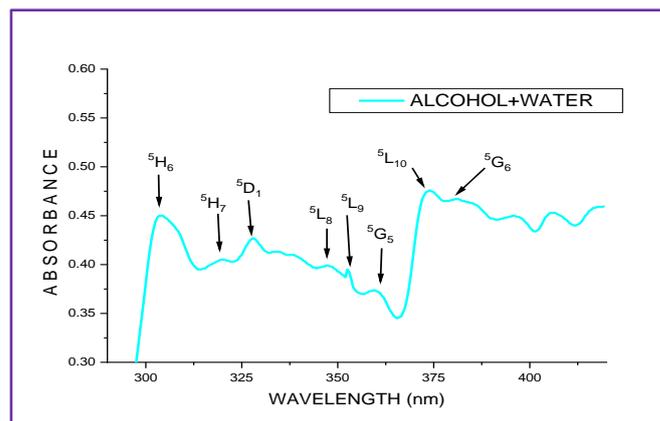
Figure 1: UV-Visible Absorption spectra of Tb(III)-I3CA Complex in non-micellar medium (ALCOHOL+WATER)
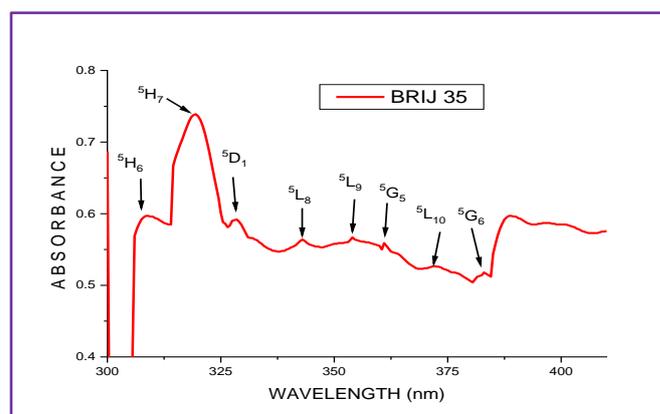
Figure 2: UV-Visible Absorption spectra of Tb(III)-I3CA Complex in micellar medium (BRIJ35)
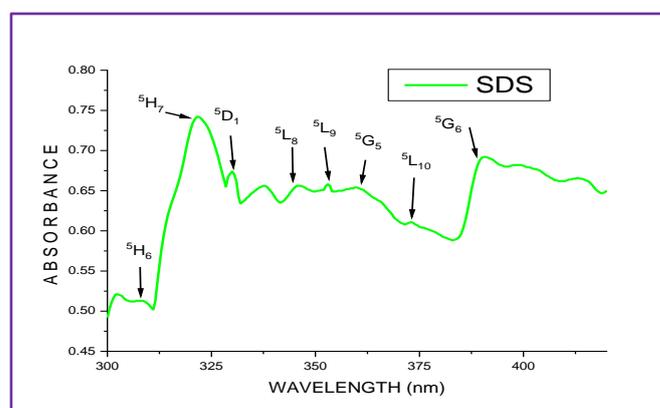
Figure 3: UV-Visible Absorption spectra of Tb(III)-I3CA Complex in micellar medium (SDS)
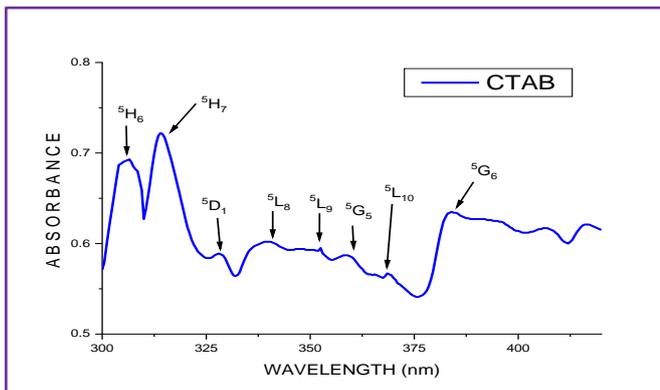
Figure 4: UV-Visible Absorption spectra of Tb(III)-I3CA Complex in micellar medium (CTAB)

Figure 5: UV-Visible Absorption spectra of Tb(III)-3ATI Complex in non-micellar medium (ALCOHOL+WATER)

Figure 6: UV-Visible Absorption spectra of Tb(III)-3ATI Complex in micellar medium (BRIJ35)
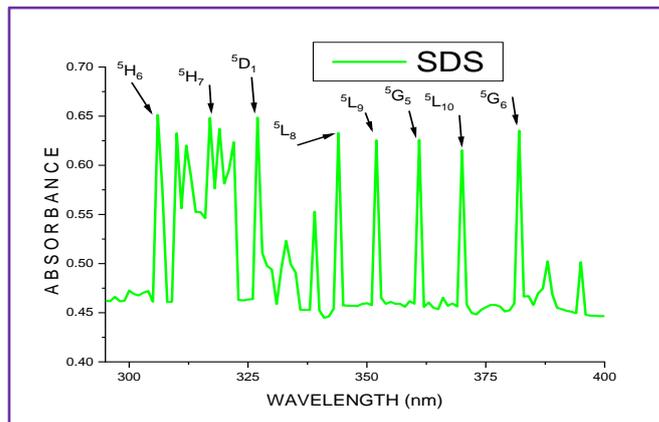
Figure 7: UV-Visible Absorption spectra of Tb(III)-3ATI Complex in micellar medium (SDS)
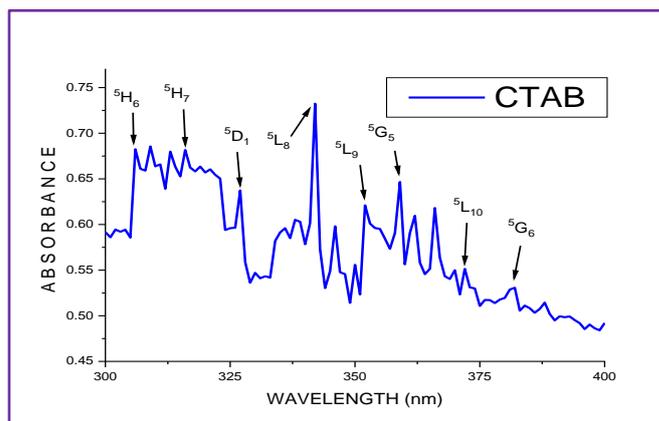
Figure 8: UV-Visible Absorption spectra of Tb(III)-3ATI Complex in micellar medium (CTAB)
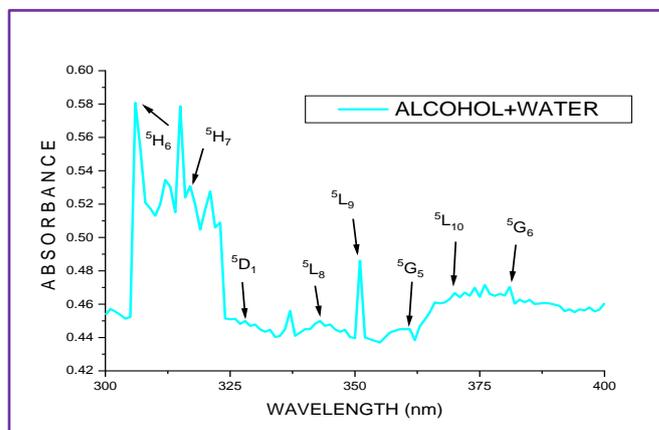
Figure 9: UV-Visible Absorption spectra of Tb(III)-I3CD Complex in non-micellar medium (ALCOHOL+WATER)
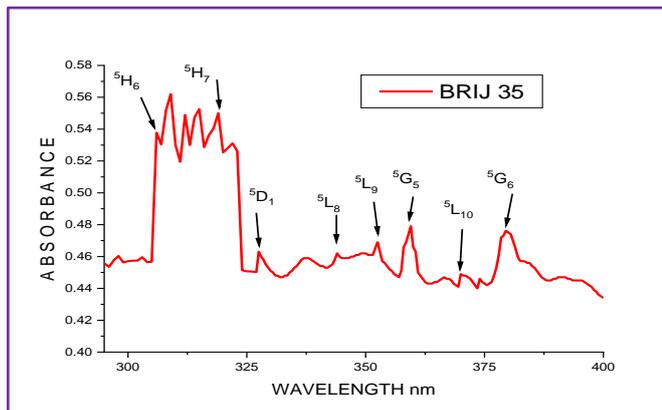
Figure 10: UV-Visible Absorption spectra of Tb(III)-I3CD Complex in micellar medium (BRIJ35)
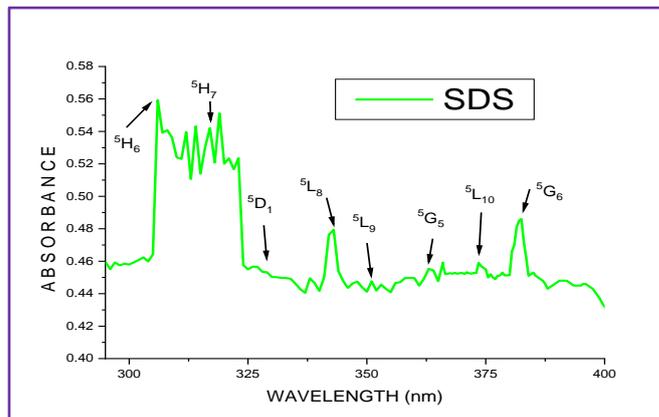
Figure 11: UV-Visible Absorption spectra of Tb(III)-I3CD Complex in micellar medium (SDS)
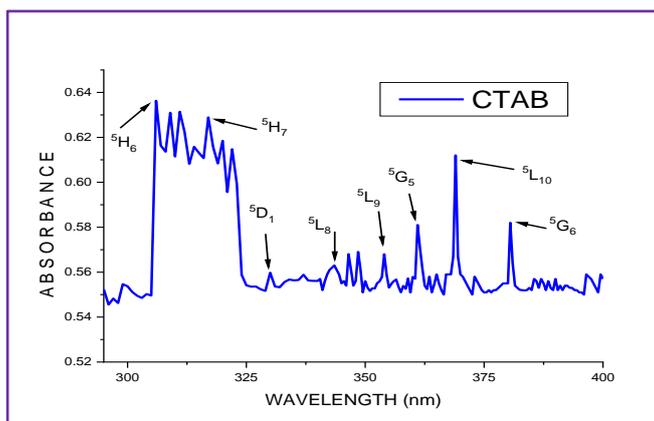
Figure 12: UV-Visible Absorption spectra of Tb(III)-I3CD Complex in micellar medium (CTAB)

7. Relative order of different Parameters in downturn sequence of Tb(III)-Complexes Doped Systems

(7.1) Intensity parameters

(a) Oscillator Strength (P) of different *f-f* transition bands or Peaks

$^5H_6 \leftarrow {}^7F_6$ Transition
Tb(III)-I3CA (BRIJ35) > Tb(III)-I3CA (CTAB) > Tb(III)-I3CA (SDS) > Tb(III)-I3CA(ALCOHOL+WATER)> Tb(III)-I3CD (ALCOHOL+WATER) > Tb(III)-I3CD (CTAB) > Tb(III)-3ATI (BRIJ35) > Tb(III)-3ATI (SDS) > Tb(III)-I3CD (BRIJ35) > Tb(III)-I3CD (SDS) > Tb(III)-3ATI (ALCOHOL+WATER) > Tb(III)-3ATI (CTAB)

$^5H_7 \leftarrow {}^7F_6$ Transition
Tb(III)-I3CA (BRIJ35) > Tb(III)-I3CA (SDS) > Tb(III)-I3CA (CTAB) > Tb(III)-I3CA (ALCOHOL+WATER) > Tb(III)-3ATI (BRIJ35) > Tb(III)-I3CD (BRIJ35) > Tb(III)-3ATI (SDS) > Tb(III)-3ATI (CTAB) > Tb(III)-I3CD (ALCOHOL+WATER) > Tb(III)-3ATI (ALCOHOL+WATER) > Tb(III)-I3CD (CTAB) > Tb(III)-I3CD (SDS)

$^5D_1 \leftarrow {}^7F_6$ Transition
Tb(III)-I3CA (CTAB) > Tb(III)-I3CA (BRIJ35) > Tb(III)-3ATI (BRIJ35) > Tb(III)-3ATI (ALCOHOL+WATER) > Tb(III)-I3CD (CTAB) > Tb(III)-I3CA (SDS) > Tb(III)-3ATI (CTAB) > Tb(III)-I3CA (ALCOHOL+WATER) > Tb(III)-3ATI (SDS) > Tb(III)-I3CD (SDS) > Tb(III)-I3CD (ALCOHOL+WATER) > Tb(III)-I3CD (BRIJ35)

$^5L_8 \leftarrow {}^7F_6$ Transition
Tb(III)-I3CA (BRIJ35) > Tb(III)-I3CA (CTAB) > Tb(III)-I3CA (SDS) > Tb(III)-I3CD (BRIJ35) > Tb(III)-3ATI (CTAB) > Tb(III)-I3CD (SDS) > Tb(III)-I3CD (CTAB) > Tb(III)-I3CD (ALCOHOL+WATER) > Tb(III)-3ATI (BRIJ35) > Tb(III)-3ATI (SDS) > Tb(III)-3ATI (ALCOHOL+WATER) > Tb(III)-I3CA (ALCOHOL+WATER)

$^5L_9 \leftarrow {}^7F_6$ Transition
Tb(III)-I3CA (BRIJ35) > Tb(III)-I3CA (CTAB) > Tb(III)-I3CD (BRIJ35) > Tb(III)-I3CD (ALCOHOL+WATER) > Tb(III)-I3CD (CTAB) > Tb(III)-3ATI (ALCOHOL+WATER) > Tb(III)-3ATI (SDS) > Tb(III)-I3CD (SDS) > Tb(III)-3ATI (BRIJ35) > Tb(III)-I3CA (ALCOHOL+WATER) > Tb(III)-3ATI (CTAB) > Tb(III)-I3CA (SDS)

$^5G_5 \leftarrow {}^7F_6$ Transition
Tb(III)-I3CA (CTAB) > Tb(III)-I3CD (ALCOHOL+WATER) > Tb(III)-I3CD (BRIJ35) > Tb(III)-I3CD (SDS) > Tb(III)-3ATI (CTAB) > Tb(III)-I3CD (CTAB) > Tb(III)-3ATI (SDS) > Tb(III)-3ATI (BRIJ35) > Tb(III)-I3CA (SDS) > Tb(III)-I3CA (BRIJ35) > Tb(III)-3ATI (ALCOHOL+WATER) > Tb(III)-I3CA (ALCOHOL+WATER)

$^5L_{10} \leftarrow {}^7F_6$ Transition
Tb(III)-I3CA (ALCOHOL+WATER) > Tb(III)-I3CA (CTAB) > Tb(III)-3ATI (BRIJ35) > Tb(III)-I3CD (CTAB) > Tb(III)-I3CD (BRIJ35) > Tb(III)-3ATI (CTAB) > Tb(III)-I3CD (ALCOHOL+WATER) > Tb(III)-I3CA (SDS) > Tb(III)-I3CD (SDS) > Tb(III)-3ATI (ALCOHOL+WATER) > Tb(III)-3ATI (SDS) > Tb(III)-I3CA (BRIJ35)

$^5G_6 \leftarrow {}^7F_6$ Transition
Tb(III)-I3CA (SDS) > Tb(III)-I3CA (BRIJ35) > Tb(III)-I3CA (CTAB) > Tb(III)-I3CA (ALCOHOL+WATER) > Tb(III)-3ATI (BRIJ35) > Tb(III)-I3CD (BRIJ35) > Tb(III)-I3CD (CTAB) > Tb(III)-I3CD (ALCOHOL+WATER)> Tb(III)-I3CD (SDS) > Tb(III)-3ATI (CTAB) > Tb(III)-3ATI (SDS) > Tb(III)-3ATI (ALCOHOL+WATER)

(b) Jodd Ofelt Parameter for each doped system

Parameter- T_2
Tb(III)-I3CA (SDS) > Tb(III)-I3CA (BRIJ35) > Tb(III)-I3CA (ALCOHOL+WATER) > Tb(III)-I3CA (CTAB) > Tb(III)-3ATI (SDS) > Tb(III)-3ATI (BRIJ35) > Tb(III)-I3CD (ALCOHOL+WATER) > Tb(III)-I3CD (BRIJ35) > Tb(III)-3ATI (ALCOHOL+WATER) > Tb(III)-3ATI (CTAB) > Tb(III)-I3CD (CTAB) > Tb(III)-I3CD (SDS)

Parameter- T_4
Tb(III)-I3CD (BRIJ35) > Tb(III)-I3CA (SDS) > Tb(III)-I3CD (SDS) > Tb(III)-3ATI (ALCOHOL+WATER)> Tb(III)-I3CD (ALCOHOL+WATER) > Tb(III)-3ATI (BRIJ35) > Tb(III)-I3CD (CTAB) > Tb(III)-I3CA (ALCOHOL+WATER) > Tb(III)-3ATI (SDS) > Tb(III)-I3CA (BRIJ35) > Tb(III)-3ATI (CTAB) > Tb(III)-I3CA (CTAB)

Parameter- T_6
Tb(III)-I3CA (ALCOHOL+WATER) > Tb(III)-I3CD (BRIJ35) > Tb(III)-3ATI (BRIJ35) > Tb(III)-I3CD (ALCOHOL+WATER) > Tb(III)-I3CA (BRIJ35) > Tb(III)-3ATI (CTAB) > Tb(III)-I3CD (CTAB) > Tb(III)-3ATI (SDS) > Tb(III)-3ATI (ALCOHOL+WATER) > Tb(III)-I3CA (CTAB) > Tb(III)-I3CD (SDS) > Tb(III)-I3CA (SDS)

(c) Root Mean Square (r.m.s) deviation-Oscillator Strength (P_{obs} & P_{cal})
Tb(III)-I3CA (BRIJ35) > Tb(III)-I3CA (CTAB) > Tb(III)-I3CA (SDS) > Tb(III)-I3CD (CTAB) > Tb(III)-3ATI (BRIJ35) > Tb(III)-I3CD (ALCOHOL+WATER) > Tb(III)-I3CD (SDS) > Tb(III)-I3CD (BRIJ35) > Tb(III)-3ATI (CTAB) > Tb(III)-I3CA (ALCOHOL+WATER) > Tb(III)-3ATI (SDS) > Tb(III)-3ATI (ALCOHOL+WATER)

(7.2) Covalency Parameters for each doped system

(a) Nephelauxetic ratio (β)-significant lower value
Tb(III)-I3CA (SDS) > Tb(III)-I3CA (BRIJ35) > Tb(III)-I3CD (SDS) > Tb(III)-I3CD (CTAB) > Tb(III)-I3CA (ALCOHOL+WATER) > Tb(III)-I3CD(BRIJ35) > Tb(III)-3ATI (SDS) > Tb(III)-3ATI (BRIJ35) > Tb(III)-I3CD(ALCOHOL+WATER) >Tb(III)-3ATI (ALCOHOL+WATER) > Tb(III)-3ATI (CTAB) > Tb(III)-I3CA (CTAB)

(b) Bonding Parameters ($b^{1/2}$)
Tb(III)-I3CA (SDS) > Tb(III)-I3CA (BRIJ35) > Tb(III)-I3CD (SDS) > Tb(III)-I3CD (CTAB) > Tb(III)-I3CA (ALCOHOL+WATER) > Tb(III)-I3CD (BRIJ35) > Tb(III)-3ATI (SDS) > Tb(III)-3ATI (BRIJ35) > Tb(III)-I3CD (ALCOHOL+WATER) > Tb(III)-3ATI (ALCOHOL+WATER) > Tb(III)-3ATI (CTAB) > Tb(III)-I3CA (CTAB)

(c) Sinha's Covalency Parameters (δ %)
Tb(III)-I3CA (SDS) > Tb(III)-I3CA (BRIJ35) > Tb(III)-I3CD (SDS) > Tb(III)-I3CD (CTAB) > Tb(III)-I3CA (ALCOHOL+WATER) > Tb(III)-I3CD (BRIJ35) > Tb(III)-3ATI (SDS) > Tb(III)-3ATI (BRIJ35) > Tb(III)-I3CD (ALCOHOL+WATER)> Tb(III)-3ATI (ALCOHOL+WATER) > Tb(III)-3ATI (CTAB) > Tb(III)-I3CA (CTAB)

(d) Covalency angular overlap Parameter (η)
Tb(III)-I3CA (SDS) > Tb(III)-I3CA (BRIJ35) > Tb(III)-I3CD (SDS) > Tb(III)-I3CD (CTAB) > Tb(III)-I3CA (ALCOHOL+WATER) > Tb(III)-I3CD (BRIJ35)> Tb(III)-3ATI (SDS) > Tb(III)-3ATI (BRIJ35) > Tb(III)-I3CD (ALCOHOL+WATER)> Tb(III)-3ATI (ALCOHOL+WATER) > Tb(III)-3ATI (CTAB) > Tb(III)-I3CA (CTAB)

(7.3) Coordination and Symmetry Parameter of each doped system

(a) Coordination Parameter – Ratio of Judd Ofelt Parameters T_4/T_2
Tb(III)-I3CD (BRIJ35) > Tb(III)-I3CD (SDS) > Tb(III)-3ATI (ALCOHOL+WATER) > Tb(III)-I3CD (CTAB) > Tb(III)-I3CD (ALCOHOL+WATER) > Tb(III)-3ATI (CTAB) > Tb(III)-I3CA (SDS) > Tb(III)-3ATI(BRIJ35) > Tb(III)-3ATI(SDS)> Tb(III)-I3CA (ALCOHOL+WATER) > Tb(III)-I3CA (CTAB) > Tb(III)-I3CA (BRIJ35)

(b) Symmetry Parameter – Ratio of Judd Ofelt Parameters T_4/T_6
Tb(III)-I3CA (SDS) > Tb(III)-I3CD (SDS) > Tb(III)-I3CD (BRIJ35) > Tb(III)-3ATI (ALCOHOL+WATER) > Tb(III)-I3CA (CTAB) > Tb(III)-3ATI (SDS) > Tb(III)-I3CD (CTAB) > Tb(III)-I3CD (ALCOHOL+WATER) > Tb(III)-3ATI (BRIJ35) > Tb(III)-I3CA (BRIJ35) > Tb(III)-3ATI (CTAB) > Tb(III)-I3CA (ALCOHOL+WATER).

Table-1 Values of experimental P_{exp} x 10^6 and theoretically P_{cal} x 10^6 Oscillator Strength of $^5H_6$, $^5H_7$, $^5D_1$, $^5L_8 \leftarrow {}^7F_6$ transitions obtained in non-micellar (Alcohol+Water) and micellar medium (BRIJ35, SDS, CTAB) for Tb(III)-Indole derivative doped system

S. No.	LEVELS	$^5H_6$		$^5H_7$		$^5D_1$		$^5L_8$	
	Tb(III)-INDOLE DERIVATIVE DOPED SYSTEMS	P_{exp}	P_{cal}	P_{exp}	P_{cal}	P_{exp}	P_{cal}	P_{exp}	P_{cal}
1	Tb(III)-I3CA (ALCOHOL+WATER)	8.5222509	3.1503996	6.5545081	5.7596418	3.1559706	0.0182419	1.1782274	1.3599261
2	Tb(III)-I3CA (BRIJ 35)	13.0497224	4.0901734	17.2581794	8.5594690	7.0295071	0.0049471	12.1947486	0.3722786
3	Tb(III)-I3CA (SDS)	8.7766005	4.8267491	14.9241752	10.5713996	3.5898669	0.0000924	6.9914003	0.0216353
4	Tb(III)-I3CA (CTAB)	10.2050134	2.0061910	13.0312556	4.2809254	7.3209370	0.0008064	9.4035425	0.0610802
5	Tb(III)-3ATI (ALCOHOL+WATER)	2.8939225	0.3287193	4.0291326	0.7226789	3.8036330	0.0020535	2.6856822	0.1593217
6	Tb(III)-3ATI (BRIJ35)	5.9064785	1.0593444	5.2838262	1.9498846	4.6324836	0.0068670	3.0308300	0.5141548
7	Tb(III)-3ATI (SDS)	5.4684119	1.0728193	4.6756815	2.2237421	2.6246605	0.0020688	2.7627070	0.1558788
8	Tb(III)-3ATI (CTAB)	2.5564187	0.4268361	4.4528930	0.6796064	3.3993611	0.0049519	4.3165425	0.3711507
9	Tb(III)-I3CD (ALCOHOL+WATER)	6.2708700	0.8563757	4.4212639	1.5415600	2.3251082	0.0068444	3.6348269	0.5154344
10	Tb(III)-I3CD (BRIJ35)	4.5682569	0.8414053	5.2751818	2.2038223	2.2009216	0.0112411	4.5861810	0.8863125
11	Tb(III)-I3CD (SDS)	4.1308562	0.1770771	3.6223292	0.5001246	2.4378001	0.0002605	4.0736132	0.0260798
12	Tb(III)-I3CD (CTAB)	6.0180548	0.3778880	3.9857968	0.6430113	3.7188765	0.0039871	3.9183471	0.3018546

Table-2 Values of experimental P_{exp} x 10^6 and theoretically P_{cal} x 10^6 Oscillator Strength of $^6I_{11/2}$, $^6I_{9/2}$, $^6I_{7/2}$, $^6P_{5/2} \leftarrow ^8S_{7/2}$ transitions obtained in non-micellar (Alcohol+Water) and micellar medium (BRIJ35, SDS, CTAB) for Tb(III)-Indole

S. No.	LEVELS Tb(III)-INDOLE DERIVATIVE DOPED SYSTEMS	$^5L_9$		$^5G_5$		$^5L_{10}$		$^5G_6$		r.m.s dev. ±σ x 10^6
		P_{exp}	P_{cal}	P_{exp}	P_{cal}	P_{exp}	P_{cal}	P_{exp}	P_{cal}	
1	Tb(III)-I3CA (ALCOHOL+WATER)	2.1736709	2.6727723	1.3842213	1.6462982	7.7638459	3.1705907	6.1477530	1.8393201	3.1493120
2	Tb(III)-I3CA (BRIJ 35)	13.9574730	0.7362297	2.0320848	1.6889568	1.9588627	0.8709500	8.1411668	2.1714999	8.3426300
3	Tb(III)-I3CA (SDS)	1.8852452	0.3173944	2.3754435	2.0889615	4.4392471	0.0706806	8.4834224	3.0387060	4.2907113
4	Tb(III)-I3CA (CTAB)	7.4948431	0.1293192	9.1597281	0.7884387	7.2148572	0.1438257	7.9130225	1.0418474	7.9545336
5	Tb(III)-3ATI (ALCOHOL+WATER)	3.1504516	0.4196860	1.4623888	0.2749326	3.1007822	0.3812940	3.1564965	0.4291349	2.7849744
6	Tb(III)-3ATI (BRIJ35)	2.2957323	1.0350489	2.3941920	0.5972450	6.5656820	1.2037018	5.5402371	0.6962119	3.8628618
7	Tb(III)-3ATI (SDS)	3.0663246	0.3268163	2.5418314	0.4771530	2.9220100	0.3659243	3.5314047	0.6197689	2.8676162
8	Tb(III)-3ATI (CTAB)	2.1654305	0.7311055	2.9069624	0.2939713	4.6160878	0.8619427	3.5781231	0.3029853	3.1536901
9	Tb(III)-I3CD (ALCOHOL+WATER)	4.1281267	1.0496678	6.0027253	0.5331971	4.5511954	1.2074615	3.5986975	0.6198938	3.7443437
10	Tb(III)-I3CD (BRIJ35)	5.2926041	2.6059110	5.7379351	1.4146711	4.9016694	2.1390484	5.1220136	2.5100293	3.2048765
11	Tb(III)-I3CD (SDS)	2.4371717	0.1713986	3.4356425	0.1831775	3.2132620	0.0692712	3.5904926	0.3549892	3.2359325
12	Tb(III)-I3CD (CTAB)	3.2592803	0.6141777	2.6366386	0.2695363	4.9349320	0.7113236	4.7674798	0.3092627	3.8758778

derivative doped systems.

Table-3 Values of **Judd Ofelt Parameters T_λ** and their ratio obtained in non-micellar (Alcohol+Water) and micellar medium (BRIJ35, SDS, CTAB) for Tb(III)-Indole derivative (I3CA, 3ATI, I3CD) doped systems.

S.NO.	Tb(III)-INDOLE DERIVATIVE DOPED SYSTEMS	T_2x10^{10}	T_4x10^{10}	T_6x10^{10}	T_4/T_2	T_4/T_6
1	Tb(III)-I3CA (ALCOHOL+WATER)	261.637451	4.793811147	19.94447329	0.018322343	0.240357871
2	Tb(III)-I3CA (BRIJ 35)	441.3029936	3.899494048	5.417089793	0.008836319	0.719850362
3	Tb(III)-I3CA (SDS)	549.2388943	50.87094394	0.101612806	0.092620797	500.6351665
4	Tb(III)-I3CA (CTAB)	223.2541146	2.020558293	0.881613794	0.009050486	2.291885979
5	Tb(III)-3ATI (ALCOHOL+WATER)	26.80957471	20.47915018	2.238273961	0.763874489	9.149527958
6	Tb(III)-3ATI (BRIJ35)	84.73679772	7.152274535	7.484976436	0.084405769	0.955550708
7	Tb(III)-3ATI (SDS)	111.0628958	4.741315487	2.254990812	0.042690364	2.102587497
8	Tb(III)-3ATI (CTAB)	23.18633073	2.773640858	5.397520914	0.119623967	0.51387311
9	Tb(III)-I3CD (ALCOHOL+WATER)	62.13433192	9.388765892	7.48319694	0.151104319	1.254646372
10	Tb(III)-I3CD (BRIJ35)	38.09222096	165.1101143	12.2715101	4.334483789	13.45475112
11	Tb(III)-I3CD (SDS)	18.73533599	22.30760538	0.285728436	1.190670153	78.07275226
12	Tb(III)-I3CD (CTAB)	22.4302685	6.210068472	4.385788939	0.276861085	1.415952422

Table-4 Values of **Bonding Parameters [β, b$^{1/2}$, δ% and η]** Computed in non-micellar (Alcohol+Water) and micellar medium (BRIJ35, SDS, CTAB) for Tb(III)-Indole derivative (I3CA, 3ATI, I3CD) doped system

S.No.	Tb(III)-INDOLE DERIVATIVE DOPED SYSTEMS	β	b$^{1/2}$	δ	η
1	Tb(III)-I3CA (ALCOHOL+WATER)	0.992032025	0.063118836	0.803197357	0.004007955
2	Tb(III)-I3CA (BRIJ 35)	0.988966293	0.074275524	1.1156808	0.005562931
3	Tb(III)-I3CA (SDS)	0.987408443	0.079345941	1.275212577	0.006355864
4	Tb(III)-I3CA (CTAB)	0.995271247	0.048624855	0.475122034	0.002372795
5	Tb(III)-3ATI (ALCOHOL+WATER)	0.994138802	0.054135009	0.589575464	0.002943545
6	Tb(III)-3ATI (BRIJ35)	0.993784804	0.055745832	0.625406585	0.003122159
7	Tb(III)-3ATI (SDS)	0.993182794	0.058383243	0.68639994	0.003426131
8	Tb(III)-3ATI (CTAB)	0.994217495	0.05377037	0.581613722	0.002903852
9	Tb(III)-I3CD (ALCOHOL+WATER)	0.994093355	0.05434448	0.594174072	0.00296647
10	Tb(III)-I3CD (BRIJ35)	0.992836258	0.059848736	0.721543196	0.003601232
11	Tb(III)-I3CD (SDS)	0.991300318	0.065953325	0.87760308	0.00437843
12	Tb(III)-I3CD (CTAB)	0.991789547	0.06407204	0.82784222	0.00413068

8. Conclusion

The optical absorption investigation of complexes in various solvent systems confirmed the interaction among metal and ligand doped systems as the principal consequences. The presence of micellar system provided the better opportunity to doped system as Tb and indole derivative ligands for more interaction among these species. Three parameters *viz:* Enhancement of P_{exp} Oscillator strength and ε_{max}, positive sign of Judd Ofelt parameters and remarkable value of covalency parameters illustrated the interaction of Tb(III) with indole derivative in spectral study.

Eight multiplet to multiplet transition bands in optical absorption spectra originated from $^7F_6$ ground state were obtained as $^5H_6 \leftarrow ^7F_6$, $^5H_7 \leftarrow ^7F_6$, $^5D_1 \leftarrow ^7F_6$, $^5L_{8,} \leftarrow ^7F_6$, $^5L_9 \leftarrow ^7F_6$, $^5G_5 \leftarrow ^7F_6$, $^5L_{10} \leftarrow ^7F_6$, $^5G_6 \leftarrow ^7F_6$ for Tb(III) ion with three indole derivatives among which $^5H_7 \leftarrow ^7F_6$ transition was hypersensitive transition. This transition exhibited high oscillator strength in complexes of Tb(III)-I3CA in BRIJ35. The electric quadrupolar selection rule was applied for $^5H_7 \leftarrow ^7F_6$ this hypersensitive transition. A strong relationship was established in between matrix element of particular *f-f* transition and obtained oscillator strength of that transition.

Oscillator strength highest in magnitude was found for Tb(III)-I3CA in BRIJ35 micellar medium. Micellar medium rather non-micellar was found better medium to enhancement in ε_{max} and oscillator strength of doped systems. Maximum red shift as Nephelauxetic ratio (β) was ascertained for Tb(III)-I3CA in SDS micellar medium, confirmed maximum metal-ligand interaction for this doped system.

Significance of T_2 Judd Ofelt parameter become more prominent as it exhibited positive sign for all micellar systems. Same coordination environment nearby the Tb(III) metal ion was assigned by Coordination T_4/T_2 parameter. High variation in symmetry T_4/T_6 parameter value inferred that the symmetry of central metal Tb(III) ion has been changed after interaction with the indole derivative in different medium. Symmetry of Tb(III) ion shown greater variation in micellar medium.

Tb(III) ion and Indole derivatives in micellar medium shown the higher covalency character. Maximum covalency character was assigned by all four covalency parameters β, $b^{1/2}$, δ and η in the Tb(III)-I3CA in SDS anionic micellar medium while minimum covalency character assigned in Tb(III)-I3CA in CTAB cationic micellar medium.

Present work can be applied for the control release of the drugs with Terbium metal. This work can also be utilized in technologies of resolution. This study concluded that enhancement in the intensity of absorption spectra by using the different greener micellar medium was obtained on keeping constant concentration of Tb metal ions which is in the favors of Atom Economy principle of green chemistry.

References

[1] Horváth IT, Anastas PT. Introduction: green chemistry. Chemical Reviews. 2007 Jun 13;107(6):2167-8.

[2] Andraos J, Matlack AS. Introduction to green chemistry. 3rd, CRC Press, Oxon (2022).

[3] Perosa A, Zecchini F. Methods and reagents for green chemistry: an introduction. John Wiley & Sons; Tundo (2007) 105-130.

[4] Linthorst JA. An overview: origins and development of green chemistry. Foundations of chemistry. 2010 Apr;12: 55-68.

[5] Cvjetko Bubalo M, Vidović S, Radojčić Redovniković I, Jokić S. Green solvents for green technologies. Journal of Chemical Technology & Biotechnology. 2015 Sep;90 (9):1631-9.

[6] Clarke CJ, Tu WC, Levers O, Brohl A, Hallett JP. Green and sustainable solvents in chemical processes. Chemical reviews. 2018 Jan 24;118(2):747-800.

[7] Welton T. Solvents and sustainable chemistry. Proceedings of the Royal Society A: Mathematical, Physical and Engineering Sciences. 2015 Nov 8;471(2183):20150502.

[8] Gallou F, Isley NA, Ganic A, Onken U, Parmentier M. Surfactant technology applied toward an active pharmaceutical ingredient: more than a simple green chemistry advance. Green Chemistry. 2016;18(1):14-9.

[9] Swatloski RP, Holbrey JD, Rogers RD. Ionic liquids are not always green: hydrolysis of 1-butyl-3-methylimidazolium hexafluorophosphate. Green Chemistry. 2003;5(4):361-3.

[10] Gompa TP, Ramanathan A, Rice NT, La Pierre HS. The chemical and physical properties of tetravalent lanthanides: Pr, Nd, Tb, and Dy. Dalton Transactions. 2020;49(45):15945-87.

[11] Mahmudov KT, Huseynov FE, Aliyeva VA, Guedes da Silva MF, Pombeiro AJ. Noncovalent interactions at lanthanide complexes. Chemistry–A European Journal. 2021 Oct 19;27(58):14370-89.

[12] Singh P, Kachhap S, Singh P, Singh SK. Lanthanide-based hybrid nanostructures: Classification, synthesis, optical properties, and multifunctional applications. Coordination Chemistry Reviews. 2022 Dec 1;472:214795.

[13] Pavel CC, Marmier A, Tzimas E, Schleicher T, Schüler D, Buchert M, Blagoeva D. Critical raw materials in lighting applications: Substitution opportunities and implication on their demand. physica status solidi (a). 2016 Nov;213(11):2937-46.

[14] Gupta I, Singh S, Bhagwan S, Singh D. Rare earth (RE) doped phosphors and their emerging applications: A review. Ceramics international. 2021 Jul 15;47(14):19282-303.

[15] Guan H, Sheng Y, Song Y, Zheng K, Xu C, Xie X, Dai Y, Zou H. White light-emitting, tunable color luminescence, energy transfer and paramagnetic properties of terbium and samarium doped BaGdF 5 multifunctional nanomaterials. RSC advances. 2016;6(77):73160-9.

[16] Heo JH, Shin DH, Park JK, Kim DH, Lee SJ, Im SH. High-performance next-generation perovskite nanocrystal scintillator for nondestructive X-ray

imaging. Advanced Materials. 2018 Oct;30(40):1801743.

[17] Binnemans K, Jones PT, Müller T, Yurramendi L. Rare earths and the balance problem: how to deal with changing markets ?. Journal of Sustainable Metallurgy. 2018 Mar;4:126-46.

[18] Zhang Z, Zheng Z. Nanostructured and/or nanoscale lanthanide metal-organic frameworks. Lanthanide Metal-Organic Frameworks. 2015:297-367.

[19] Clear KJ. Molecular probes for bio membrane recognition. University of Notre Dame; 2016.

[20] Abu Elgoud EM, Ismail ZH, Ahmad MI, El-Nadi YA, Abdelwahab SM, Aly HF. Sorption of lanthanum (III) and neodymium (III) from concentrated phosphoric acid by strongly acidic cation exchange resin (SQS-6). Russian journal of applied chemistry. 2019 Nov;92:1581-92.

[21] Kamal R, Saif M. Barium tungstate doped with terbium ion green nanophosphor: Low temperature preparation, characterization and potential applications. Spectrochimica Acta Part A: Molecular and Biomolecular Spectroscopy. 2020 Mar 15;229:117928.

[22] Radwan MA, Ragab EA, Sabry NM, El-Shenawy SM. Synthesis and biological evaluation of new 3-substituted indole derivatives as potential anti-inflammatory and analgesic agents. Bioorganic & medicinal chemistry. 2007 Jun 1;15(11):3832-41.

[23] Kaushik NK, Kaushik N, Attri P, Kumar N, Kim CH, Verma AK, Choi EH. Biomedical importance of indoles. Molecules. 2013 Jun 6;18(6):6620-62.

[24] Rossiter S, Folkes LK, Wardman P. Halogenated indole-3-acetic acids as oxidatively activated prodrugs with potential for targeted cancer therapy. Bioorganic & medicinal chemistry letters. 2002 Sep 16;12(18):2523-6.

[25] Jørgensen CK, Judd BR. Hypersensitive pseudo quadrupole transitions in lanthanides. Molecular Physics. 1964 Jan 1;8(3):281-90.

[26] Ishikawa N, Iino T, Kaizu Y. Interaction between f-electronic systems in binuclear lanthanide complexes with phthalocyanines. Journal of the American Chemical Society. 2002 Sep 25;124(38):11440-7.

[27] Ahmed Z, Iftikhar K. Efficient layers of emitting ternary lanthanide complexes for fabricating red, green, and yellow OLEDs. Inorganic chemistry. 2015 Dec 7;54(23):11209-25.

[28] Debnath GH, Chakraborty A, Ghatak A, Mandal M, Mukherjee P. Controlled terbium (III) luminescence in zinc sulfide nanoparticles: an assessment of competitive photophysical processes. The Journal of Physical Chemistry C. 2015 Oct 22;119(42):24132-41.

[29] Zhao YW, Zhang FQ, Zhang XM. Single component lanthanide hybrids based on metal–organic framework for near-ultraviolet white light LED. ACS Applied Materials & Interfaces. 2016 Sep 14;8(36):24123-30.

[30] Pan G, Bai X, Yang D, Chen X, Jing P, Qu S, Zhang L, Zhou D, Zhu J, Xu W, Dong B. Doping lanthanide into perovskite nanocrystals: highly improved and expanded optical properties. Nano letters. 2017 Dec 13;17(12):8005-11.

[31] Loiko P, Volokitina A, Mateos X, Dunina E, Kornienko A, Vilejshikova E, Aguilo M, Diaz F. Spectroscopy of Tb3+ ions in monoclinic KLu (WO4) 2 crystal

[32] Liu B, Shi J, Wang Q, Tang H, Liu J, Zhao H, Li D, Liu J, Xu X, Wang Z, Xu J. Crystal growth, polarized spectroscopy and Judd-Ofelt analysis of Tb: YAlO3. Spectrochimica Acta Part A: Molecular and Biomolecular Spectroscopy. 2018 Jul 5;200:58-62.

[33] Subrahmanyam T, Gopal KR, Suvarna RP, Jamalaiah BC, Kumar MV. Luminescent properties of Tb3+-doped TeO2-WO3-GeO2 glasses for green laser applications. Optical Materials. 2018 Jun 1;80:154-9.

[34] Carnall WT, Fields PR, Wybourne BG. Spectral intensities of the trivalent lanthanides and actinides in solution. I. Pr3+, Nd3+, Er3+, Tm3+, and Yb3+. The Journal of Chemical Physics. 1965 Jun 1;42(11):3797-3806.

[35] Carnall WT, Fields PR, Rajnak K. Spectral intensities of the trivalent lanthanides and actinides in solution. II. Pm3+, Sm3+, Eu3+, Gd3+, Tb3+, Dy3+, and Ho3+. The journal of chemical physics. 1968 Nov 15;49(10):4412-23.

[36] Judd BR. Optical absorption intensities of rare-earth ions. Physical review. 1962 Aug 1;127(3):750.

[37] Ofelt GS. Intensities of crystal spectra of rare-earth ions. The journal of chemical physics. 1962 Aug 1;37(3):511-20.

[38] Carnall WT, Beitz JV, Crosswhite H, Rajnak K, Mann JB. Systematics and the Properties of the Lanthanides. Ch. 1983;9:389-450.

[39] Henrie DE, Choppin GR. Environmental effects on f–f transitions. II.“hypersensitivity” in some complexes of trivalent neodymium. The Journal of Chemical Physics. 1968 Jul 15;49(2):477-81.

[40] Sinha SP. Spectroscopic investigations of some neodymium complexes. Spectrochimica Acta. 1966 Jan 1;22(1):57-62.

[41] Goutam MP, Yadav A, Limaye SN. Electronic spectral studies on mixed ligand complexes of some biologically active elements Pr (III) and Nd (III) involving histidine as primary ligand and ninhydrin as secondary ligand. Asian Journal of Chemistry. 1998 Jul 1;10(3):415.

[42] Carnall WT, Fields PR, Rajnak K. Electronic energy levels of the trivalent lanthanide aquo ions. III. Tb3+. The Journal of chemical physics. 1968 Nov 15;49(10):4447-9.

[43] Reid MF, Richardson FS. Electric dipole intensity parameters for lanthanide 4f→ 4f transitions. The Journal of chemical physics. 1983 Dec 15;79(12):5735-42.

[44] Ligner G, Mohan R, Knittel S, Duportail G. Hypersensitivity of terbium and europium ions luminescence in biological substrates. Spectrochimica Acta Part A: Molecular Spectroscopy. 1990 Jan 1;46(5):797-802.

[45] Zairov RR, Dovzhenko AP, Podyachev SN, Sudakova SN, Kornev TA, Shvedova AE, Masliy AN, Syakaev VV, Alekseev IS, Vatsouro IM, Mambetova GS. Role of PSS-based assemblies in stabilization of Eu and Sm luminescent complexes and their thermoresponsive luminescence. Colloids and Surfaces B: Bio interfaces. 2022 Sep 1;217:112664.

[46] Carnall WT, Fields PR, Rajnak K. Electronic energy levels of the trivalent lanthanide aquo ions. II. Gd3+. The

Journal of chemical physics. 1968 Nov 15;49(10):4443-6.

[47] Jørgensen CK, Reisfeld R. Judd-Ofelt parameters and chemical bonding. Journal of the Less Common Metals. 1983 Sep 1;93(1):107-12.

[48] Khatri S, Bala M, Hooda P, Ahlawat P, Khatkar SP, Taxak VB, Kumar R. Utilization of Judd-Ofelt theory to assess the photophysical properties of β-keto carboxylate Tb (III) complexes with heterocyclic secondary sensitizer. Optical Materials. 2022 Sep 1;131:112629.

[49] Terra IA, Borrero-González LJ, Almeida JM, Hernandes AC, Nunes LA. Judd-ofelt analysis of tb 3+ and up conversion study in yb 3+-tb 3+ co-doped calibo glasses. Química Nova. 2020 May 18;43:188-93.

[50] Rice NT, Popov IA, Russo DR, Bacsa J, Batista ER, Yang P, Telser J, La Pierre HS. Design, isolation, and spectroscopic analysis of a tetravalent terbium complex. Journal of the American Chemical Society. 2019 Jul 28;141(33):13222-33.

[51] Hooda A, Dalal A, Nehra K, Singh D, Kumar S, Malik RS, Kumar P. Preparation and optical investigation of green luminescent ternary terbium complexes with aromatic β-diketone. Chemical Physics Letters. 2022 May 1;794:139495.